International Journal of Nanomedicine

Dovepress

open access to scientific and medical research

Open Access Full Text Article

ORIGINAL RESEARCH

Fe-Capsaicin Nanozymes Attenuate Sepsis-Induced Acute Lung Injury via NF-κB Signaling

Ruijie Wang[1,2], Quan Li[1], Pengxin Wu[3], Ke Ren[3], Yan Li[1], Yang Wang[3], Huadong Zhu[1], Chuanzhu Lv[2–4]

[1]Emergency Department, State Key Laboratory of Complex Severe and Rare Diseases, Peking Union Medical College Hospital, Chinese Academy of Medical Science and Peking Union Medical College, Beijing, People's Republic of China; [2]Research Unit of Island Emergency Medicine, Chinese Academy of Medical Sciences (No. 2019RU013), Hainan Medical University, Haikou, People's Republic of China; [3]Emergency Medicine Center, Sichuan Provincial People's Hospital, University of Electronic Science and Technology of China, Chengdu, People's Republic of China; [4]Key Laboratory of Emergency and Trauma of Ministry of Education, Hainan Medical University, Haikou, People's Republic of China

Correspondence: Chuanzhu Lv; Huadong Zhu, Email Lvchuanzhu677@126.com; zhuhuadong1970@126.com

Background: In sepsis, the lungs are one of the most severely affected organs, usually resulting in acute lung injury (ALI). Capsaicin (CAP) is a natural compound found in chili peppers that has pain-relieving and anti-inflammatory properties. Here, we report that nanoparticles containing capsaicin and iron (Fe-CAP NPs) exhibited anti-inflammatory effects in the treatment of ALI.

Methods: The morphological characteristics of nanozymes were detected. RAW 264.7 cells were divided into four groups: control, lipopolysaccharide (LPS), CAP+LPS and Fe-CAP+LPS groups. The expression of inducible nitric oxide synthase (iNOS), transforming growth factor-β (TGF-β), and tumor necrosis factor-α (TNF-α) was assessed by immunofluorescence, Western blot, and enzyme-linked immunosorbent assay (ELISA). Nuclear factor kappa-B (NF-κB) expression was determined by Western blot. C57 mice were divided into control, LPS, CAP+LPS and Fe-CAP+LPS groups. Interleukin-6 (IL-6) and iNOS expression in the lung was detected by Western Blot. IL-6 and TNF-α expression in serum was detected by ELISA. Extravasated Evans blue, histopathological evaluation and wet-to-dry (W/D) weight ratio were used to assess pulmonary capillary permeability. The blood and major organs (heart, liver, spleen, lung and kidney) of mice were tested for the toxicity of Fe-CAP NPs.

Results: In the LPS group, TNF-α, iNOS, p-NF-κB and p-IKBα expression increased. However, their expression was significantly decreased in the Fe-CAP+LPS group. TGF-β expression showed the opposite trend. In vivo, IL-6 and iNOS expression was notably increased in the lungs of LPS group of mice but decreased with Fe-CAP pretreatment. Fe-CAP significantly ameliorated lung EB leakage, improved the histopathology of lung tissue and reduced the W/D weight ratio. The nanoparticles showed non-cytotoxicity, when studying these biological activities.

Conclusion: Fe-CAP NPs could alleviated inflammation by inhibiting the expression of pro-inflammatory factors in macrophages, increasing the expression of anti-inflammatory factors, and alleviating lung tissue damage.

Keywords: capsaicin, sepsis, macrophage, nanoparticles, iron

Introduction

Sepsis remains a prevalent condition in intensive care units(ICU) worldwide.[1] The pathogenesis of sepsis is characterised by a dysregulated host response to infection.[2] In 2017, it was reported that 48.7 million people worldwide suffered from sepsis, of which 11 million died from sepsis, accounting for 19.7% of all deaths worldwide.[3] The high mortality rate and the substantial treatment costs impose a significant burden on the global economy.[4]

Sepsis is a syndrome characterized by a dysregulated host response to invading pathogens that involves hemodynamic alterations leading to multiple life-threatening organ dysfunctions.[5] In sepsis, the lungs are particularly susceptible to damage,[6] often resulting in acute lung injury (ALI). ALI is characterised by increased pulmonary microvascular permeability triggered by the inflammatory response, disruption of the blood-gas barrier function, and excessive leakage of fluid and macromolecular substances from pulmonary capillaries into the alveolar cavities and lung interstitium.[7] These pathological changes lead to impaired oxygenation, pulmonary edema, and respiratory failure.[8] Multiple mechanisms aggravate the progression of ALI, including inflammation and oxidative stress.[9] During sepsis, resident and circulating white blood cells (WBCS) are activated

Received: 21 August 2023
Accepted: 17 December 2023
Published: 3 January 2024

and infiltrate the lungs, where they release large amounts of pro-inflammatory cytokines, such as tumor necrosis factor-α (TNF-α) and interleukin-6 (IL-6), etc. These cytokines further promote WBC activation and recruitment, which in turn aggravate lung injury. A large number of studies have shown that gram-negative bacterial infection is one of the most important causes of ALI, and lipopolysaccharides (LPS), a major component of the outer membrane of gram-negative bacteria, may cause lung injury and inflammatory responses.[10,11] At present, the LPS-induced ALI mouse model is widely used for pathogenesis research.[12] Due to the lack of effective treatment options, ALI usually develops into an extreme form of acute respiratory distress (ARDS), which has become a focus of difficult clinical work due to its high morbidity and mortality. Hence, developing a nanodrug with anti-inflammatory properties would be a promising strategy for treating ALI.

Capsaicin (CAP), the principal component of chili peppers,[13] has been utilised clinically to reduce inflammation due to its natural availability and nontoxicity.[14–16] However, due to the hydrophobicity of capsaicin, its application is limited in vivo.[17]

In recent years, nano-carriers have gained significant attention in the field of nanotechnology due to their selectivity and ability to enhance drug activity.[18–20] Nanozymes, a series of nanomaterials with enzyme-like activity, have garnered considerable interest in the biomedical field owing to their high stability and cost-effectiveness.[21–23] In this study, we developed iron-capsaicin-based nanoparticles (Fe-CAP NPs) by combining iron with the anti-inflammatory drug capsaicin, and investigated their potential for treating ALI. Our findings demonstrated that Fe-CAP NPs could reduce the expression of several important inflammatory factors, such as inducible nitric oxide synthase (iNOS) and interleukin-6 (IL-6), through the nuclear factor kappa-B (NF-κB) pathway. Furthermore, in vivo, Fe-CAP NPs exhibited significant anti-inflammatory effects, leading to near-normalization of lung tissue, suggesting that Fe-CAP NPs were highly effective in treating ALI.

Materials and Methods

Reagents and Chemicals

The following reagents were used for examination: lipopolysaccharide (LPS) (Sigma, L3129-10MG), capsaicin (MCE, 404864–50 mg), $FeCl_3$•$6H_2O$ (Aladdin, F102739-55 g), polyvinylpyrrolidone (PVP) (Aladdin, P434440-250 g), fetal bovine serum (Gibco, 30044333), DMEM culture medium (Gibco, C11995500BT), PBS (Gibco, 8123157), primary and secondary antibody dilution solution (BOSTER, 17K28C17), color pre-stained protein marker (Thermo, 26619), TNF-α (Abcam, ab66579), iNOS (Abcam, ab283655), TGF-β (Huabio, HA7211430), p-NF-κB (Cell Signaling Technology, 3033S), NF-κB (Cell Signaling Technology, 8242T), p-IKBα (Abcam, ab32518), IKBα (Abcam, ab133462), IL-6 (Huabio, R1412-2), β-actin (Cell Signaling Technology, 4970S), Pierce TM BCA protein Assay kit (Thermo Fisher Scientific, Prod # 23227), F4/80 (Huabio, RT1212), anti-rabbit IgG, HRP-linked antibody (Cell Signaling Technology, 7074S), anti-mouse IgG, HRP-linked antibody (Cell Signaling Technology, 7076S), secondary antibody (Thermo Fisher Scientific, Prod # A-31572), secondary antibody (Thermo Fisher Scientific, Prod # A-21202), SuleLumia ECL kit (Abbkine, K22020), TNF-α and iNOS ELISA kit (FineTest, EM0183, EM0272), IL-6 ELISA kit (Solarbio, SEKM-0007), Cell Counting kit-8 (CCK-8, Beyotime, C0038).

Preparation of the Fe-CAP NPs

First, 30 mg polyvinylpyrrolidone (PVP) was dissolved in 5 mL methanol, and 20 mg $FeCl_3$•$6H_2O$ dissolved in 1 mL methanol was added while stirring. After 30 min, 10 mg capsaicin dissolved in 1 mL methanol (methanol capsaicin solution required ultrasound until capsaicin was completely dissolved) was added and the mixture was stirred for 3 h. Dialysed with ultra-pure water for 72 h and changed it every 12 h. Finally, the obtained solution could be vacuum freeze-dried for subsequent experiments.

Cell Culture

RAW 264.7 cells (Meisen cell, Zhejiang, China, CTCC-001-0048) were treated with Dulbecco's modified eagle medium (DMEM, Gibco by Thermo Fisher Scientific, United States, C11995500BT) containing 10% fetal bovine serum (Fetal Bovine Serum, FBS, Gibco by Thermo Fisher Scientific, United States, 30044333) and cultured in 25 cm^2 culture bottles at 37 °C in humidified 5% CO_2/95% air. The medium was replaced every 48 h.

Cell Viability Assay

Cell Counting kit-8 (CCK-8, Beyotime, C0038) was used to detect the viability of RAW 264.7 cells. The RAW 264.7 cells (2×10^4 cells/well) were seeded onto 96-well microplates treated with CAP (capsaicin, MCE, USA) (ranging from 25 to 100 μM) and Fe-CAP (ranging from 7.5 to 30 μg/mL) for 0 h, 3 h, 6 h and 9 h. After discarding the medium, 90 μL of fresh basic medium and 10 μL of CCK-8 solution were added to each well. The cells were subsequently incubated for an additional 2 h. Then, the optical density was read at 450 nm with a microplate reader. The experiment was repeated three times.

RAW 264.7 Groups and Treatments

The RAW 264.7 cells were randomly divided into four groups: the control group, LPS group, CAP+LPS group and Fe-CAP+LPS group. Referring to relevant studies, we selected 50 μM of capsaicin to treat RAW 264.7.[24] After conversion, the concentration corresponding to 50 μM capsaicin was 15.27 μg/mL, so the concentration of Fe-CAP NPs for following experiment was 15 μg/mL. In the control group, RAW 264.7 cells were cultured with basic medium (DMEM) for 8 h. In the CAP+LPS and Fe-CAP+LPS groups, cells were respectively pretreated with CAP (50 μM) and Fe-CAP (15 μg/mL) for 2 h, followed by treatment with LPS (1 μg/mL) for 6 h. Conversely, RAW 264.7 cells in the LPS group were directly treated with LPS (1 μg/mL) for 6 h. The cells or medium in 6-well plates were then collected for subsequent protein extraction, ELISA analyses and immunofluorescence. The experiment was repeated three times.

Ethics of Animals

The use and handling of mice for sepsis or toxicity detection adhered to ethical guidelines outlined in the National Institutes of Health Guide for the Care and Use of Laboratory Animals. The use of animals and experimental protocols was approved by the Ethics Committee (Number 326, 2023) of Sichuan Province People's Hospital. Every effort was made to minimise the number of mice used and to alleviate their suffering.

Animals and Treatments

C57 mice (male, 6–8 weeks old and weighing 18–22 g) (Table 1) were obtained from Byrness Weil Biotech Ltd Corporation. All animals were given free water and standard laboratory diet. At random, mice were divided into four groups: sham, LPS (10 mg/kg, i.p.),[25] CAP (8 mg/kg, i.p.)+LPS (10 mg/kg, i.p.) and Fe-CAP (8 mg/kg, i.p.)+LPS (10 mg/kg, i.p.). Mice in the CAP+LPS group were given with CAP (8 mg/kg, i.p.) every 24 h,[26] at 96 h before injected of LPS. Similarly, in Fe-CAP+LPS group, the mice were given with Fe-CAP (8 mg/kg, i.p.) every 24 h, at 96 h before injected of LPS. All mice were euthanised 12 h after being injected with LPS.

Western Blotting

For different RAW 264.7 groups, the media was discarded and the cells were washed with 1×PBS solution more than two times. Subsequently, a lysis buffer was used to lyse the cells. The resulting cell fragments were then scraped off the plates using a rubber scraper and subjected to centrifugation at 15,000 rpm for 15 minutes to separate the supernatant. For each group of mice, the left lung was carefully preserved in liquid nitrogen at −80°C. The extraction of total proteins was performed using protein extraction reagents (Pierce, Thermo Fisher Scientific Corporation, Bloomingdale, Illinois, USA). These reagents were supplemented with protease inhibitors to ensure optimal extraction conditions.

Table 1 Number of Animals Used in Various Treatments

Usage		Control	LPS	CAP+LPS	Fe-CAP+LPS	Fe-CAP
Mouse	EB (died in 12h)	N=3	N=4(1)	N=3	N=3	
	Lung pathology, WB and W/D	N=3	N=6	N=7	N=7	
	Toxicity testing	N=5				N=15
	Immunohistochemistry	N=3	N=3	N=3	N=3	
Total		N=14	N=13(1)	N=13	N=13	N=15

BCA protein detection kit (BCA, Beyotime, P0010) was used to test the protein concentration in RAW 264.7 cells and tissues. The 40 μg protein sample was heated to 100 ° C for 10 min and separated by electrophoresis on a 10% gel using sodium dodecyl sulpho-polyacrylamide gels. The separated proteins were transferred to a polyvinylidene fluoride (PVDF) membrane. The membrane was initially blocked with 5% skim milk solution for 1 hour at room temperature. After blocking, the membrane was then incubated overnight at 4°C with appropriate primary antibodies (1:1000) and subsequently with appropriate secondary antibodies (1:5000) for 1 hour at room temperature. Immunoblots were visualised using the SuleLumia ECL kit (Abbkine, USA, K22020). Band intensity was quantified using imageJ software. Specific details about the antibodies used can be found in Table 2. The experiment was repeated a minimum of three times.

Double Immunofluorescence

RAW 264.7 cells were cultured in confocal plates for 24 h. Subsequently, the cells were treated with either CAP (50 μM) or Fe-CAP (15 μg/mL) for 2 hours, followed by stimulation with LPS (1 μg/mL) for 6 hours. Then, the cells were fixed with 4% paraformaldehyde and 0.1 M PBS at room temperature for 15 minutes. Subsequently, the cells were treated with 10% donkey serum for 1 hour to block nonspecific binding and were then washed three times with 1× PBS for 5 minutes each. Next, the cells were respectively incubated with appropriate primary antibodies overnight at 4°C and FITC/Cy3-conjugated secondary antibodies at room temperature in the dark for 1 h. Finally, DAPI was added to the plates and incubated for 10 minutes. Images were captured at 200× magnification. The experiment was performed at least three times.

Enzyme-Linked Immunosorbent Assay (ELISA)

RAW 264.7 cells were incubated in 6-well plates for 24 h. Next, the cells underwent a 2-hour pretreatment with CAP (50 μM) and Fe-CAP (15 μg/mL). Subsequently, the cells were stimulated with LPS (1 μg/mL) for another 6 h. The supernatant was collected and analysed by ELISA.

The blood of different groups of animals was collected, immobilized for 2 h and centrifuged at 3000 r for 15 min, serum was then collected for ELISA.

The standards or test samples were added to each well, the plate was covered with a plate sealer, and the plate was incubated in a incubator for 90 min at 37 °C. The plate was then washed with 1× wash buffer for 2 times. Wash buffer was then discarded, and 100 μL of biotin-labelled antibody was added to each well and the plate was incubated at 37 °C for 60 min. The plate was washed with 1× wash buffer 3 times. Afterwards, 100 μL of HRP-streptavidin conjugate

Table 2 Antibodies Used for Western Blotting and Immunofluorescence

Antibody	Host	Source	Catalog Number	Dilution for Staining	Dilution for Western Blot
TNF-α	Rabbit polyclonal	Abcam, United Kingdom	ab66579	1:200	1:1000
iNOS	Rabbit polyclonal	Abcam, United Kingdom	ab283655	1:200	1:1000
TGF-β	Rabbit polyclonal	Huabio, China	HA721143		1:500
p-NF-κB	Rabbit polyclonal	Cell Signaling Technology, United States	3033S		1:1000
NF-κB	Rabbit polyclonal	Cell Signaling Technology, United States	8242T		1:1000
p-IKBα	Rabbit polyclonal	Abcam, United Kingdom	ab32518		1:1000
IKBα	Rabbit polyclonal	Abcam, United Kingdom	ab133462		1:1000
IL-6	Rabbit polyclonal	Huabio, China	R1412-2		1:500
β-actin	Rabbit polyclonal	Cell Signaling Technology, United States	4970S		1:1000
IgG-HRP	Mouse monoclonal	Thermo Fisher Scientific, United States	7076S		1:1000
IgG-HRP	Rabbit polyclonal	Thermo Fisher Scientific, United States	7074S		1:1000
Secondary Antibody	Donkey polyclonal	Thermo Fisher Scientific, United States	A-31572	1:200	
Secondary Antibody	Donkey polyclonal	Thermo Fisher Scientific, United States	A-21202	1:200	
F4/80	Rabbit polyclonal	Huabio, China	RT1212	1:200	

(SABC) was added to each well and the plate was incubated at 37 °C for 30 min. The plate was washed with 1× wash buffer 5 times. The wash buffer was discarded, and 90 μL of TMB substrate was added to each well. Finally, 50 μL of stop solution was added to each well. The optical density was read at 450 nm with a microplate reader.

Assessment of Pulmonary Capillary Leakage

Exosmotic Evans blue (EB) was utilised to evaluate pulmonary capillary permeability. Mice were anesthetised with 3% pentobarbital sodium (30 mg/kg) 12 h after intraperitoneal injection of LPS. Subsequently, 0.5% EB solution was injected through the tail vein. Within 30 min of the EB injection, the mice were euthanised. The right lung tissue homogenate was weighed and then treated with formamide (4 mL/g (wet tissue)) for 24 h at room temperature. The sample was then centrifuged at 4000 × g for 30 min. The absorbance value of the dye was determined by an enzyme-labeled instrument (620 nm). The concentration of Evans blue was then calculated based on the absorbance obtained from the standard curve.

Histological Examination and Lung Injury Score (LIS)

At 12 h after LPS injection, the mice were anesthetised using 3% pentobarbital sodium (30 mg/kg). The right lung tissue was carefully isolated and fixed in 4% paraformaldehyde. Subsequently, the tissue was embedded in paraffin and sectioned into slices with a thickness of 4 μm. These sections were subjected to routine staining with hematoxylin-eosin (H&E). The lung injury score (LIS) was then quantified in a blinded manner.[27]

Measurement of the Lung Wet-to-Dry (W/D) Weight Ratio

The right lung was removed and dried it in an oven at 65 °C for 72 h until the lung weight no longer changed. The dry to wet weight ratio was calculated.

Collection of BALF

The lungs were irrigated with 1mL of pre-cooled PBS, and BALF was slowly collected after 1 minute. The above operation was repeated 3 times. The collected BALF was centrifuged at 1000×g at 4 °C for 10 min. The supernatant was frozen at −80 °C for later analysis. BCA protein detection kit was used to detect the total protein concentration in BALF. Inflammatory factors in BALF were detected by ELISA kit.

Immunohistochemistry (IHC)

Lung tissue was immobilized, dehydrated, embedded, sliced, and dewaxed. Subsequently, slices were closed with 3% bovine serum albumin (BSA) at room temperature and incubated overnight at 4°C with primary antibodies (TNF-α and IL-6). Then, slices were incubated with secondary and tertiary antibodies at 37°C for 20 min. The slices were then exposed to DAB substrate and stained with hematoxylin in a light-protected environment. After the dehydration and drying sequence, the slices are installed using neutral adhesive. Finally, slide evaluation was performed under a microscope.

Toxicity of Fe-CAP NPs in Mice

After intraperitoneal (i.p.) injection of Fe-CAP, mice (n=15) were sacrificed at 1, 7, and 14 days postinjection. The major organs (heart, liver, lung, spleen and kidney) were subjected to standard H&E staining protocols for histological examination. Blood samples were collected from the heart of each mouse to assess routine blood parameters as well as liver and kidney function. The main detection indicators were as follows: white blood cell (WBC), red blood cell (RBC), hemoglobin (HGB), hematocrit (HCT), mean corpuscular volume (MCV), mean corpuscular hemoglobin (MCH), mean corpuscular hemoglobin concentration (MCHC), platelets (PLT), lymphocytes (Lym), monocytes (Mon), granulocytes (Gran), plateletcrit (PCT), alanine transaminase (ALT), aspartate transaminase (AST), urea nitrogen (BUN), and creatinine (CRE).

Data Analysis

All experiments were conducted a minimum of three times. Statistical analysis was performed using GraphPad Prism 8.0 Software (GraphPad Software, San Diego, CA). After assessing the homogeneity of variance, one-way analysis of variance (ANOVA) was used, and then the multifactor comparison Tukey's test was used to determine the statistical significance between groups. When $p< 0.05$, the difference was regarded as statistically significant.

Results

Characterization of Fe-CAP NPs

Fe-CAP NPs were synthesised by adding capsaicin drops to a mixture of $FeCl_3$ and polyethylpyrrolidone (PVP) (dispersed in methanol). PVP has good water dispersibility and can promote the synthesis of nanozymes. Scanning electron microscopy (SEM) of the Fe-CAP NPs showed that the nanozyme had a good morphology (Figure 1B). Transmission electron microscopy (TEM) was used to characterise the morphology and element mapping of Fe-CAP NPs, that C, O and Fe elements coexist and evenly distributed (Figure 1B). Fe-CAP nanoparticles showed excellent stability when dispersed in water, phosphate buffered saline (PBS) (10 mM, pH 7.4), normal saline (NS), Dulbecco's modified Eagle's medium (DMEM) and fetal bovine serum (FBS) for 1 week (Figure 1C). The UV-vis absorption wavelength of the NPs was approximately 219 nm (Figure 1D). X-ray photoelectron spectroscopy (XPS) analysis revealed two strong binding energy peaks at 711 eV and 724 eV for Fe 2p3/2 and 2p1/2, respectively (Figure 1E), and the C-related bonds in capsaicin (Figure 1F). Together, these data confirmed that the iron in our nanoparticles was related to capsaicin.

Effects of CAP and Fe-CAP on Viability of RAW 264.7

The cytotoxicity of CAP and Fe-CAP on RAW 264.7 cells was determined by CCK-8 assay. Cells were treated with 25 to 100 μM CAP for 9 h (Figure 2B) and 7.5 to 30 μg/mL Fe-CAP for 9 h. The results showed that within 9 h, there were no changes in cell viability after treatment with both drugs. Subsequently, we used CAP (50 μM) or Fe-CAP (15 μg/mL) for 2 h, and LPS (1 μg/mL) for 6 h for vitro analysis.

The Anti-Inflammatory Effect of Fe-CAP NPs in LPS-Stimulated Macrophage Cells

We investigated relevant inflammatory cytokines by Western blotting assay, Enzyme-linked immunosorbent assay (ELISA) and immunofluorescence methods.

Western blot results showed that compared with the control group, the expression of the inflammatory cytokines tumor necrosis factor-α (TNF-α) (Figure 2C-2 and C-3) and iNOS (Figure 3B and C) in RAW 264.7 cells in the LPS group was increased, while Fe-CAP NPs treatment effectively reduced their expression. Similarly, the expression of the anti-inflammatory factor transforming growth factor-β (TGF-β) (Figure 3B and D) was decreased in the LPS group and significantly increased after Fe-CAP pretreatment. Notably, capsaicin itself also had anti-inflammatory effect when used alone, which could reduce the expression of inflammatory factors,[17] but it was less effective than Fe-CAP NPs. This suggested that iron and capsaicin had a synergistic effect in alleviating inflammation. Next, we found that the nuclear factor kappa-light-chain-enhancer of activated B cells (NF-κB) pathway, an important mode of cell signaling, was activated in the LPS group (Figure 3B, E and F). Nonetheless, the levels of these cytokines returned to normal after administration of Fe-CAP NPs or capsaicin, confirming the anti-inflammatory effect of Fe-CAP NPs.

The immunofluorescence results showed that Fe-CAP NPs effectively reduced the fluorescence intensity of TNF-α (Figure 2C-1) and iNOS (Figure 3A). Similar findings were observed by ELISA (Figure 3G and H). Collectively, these results suggested that Fe-CAP can reduce the expression of the inflammatory factors TNF-α and iNOS and increase the expression of TGF-β through the NF-κB pathway to alleviate inflammation.

The Anti-Inflammatory Effect of Fe-CAP NPs in the Lung Tissue of LPS-Stimulated Mice

The flow chart of the animals experiment section was depicted in Figure 4A. Western blot showed that inflammatory cytokines iNOS (Figure 4B-1 and B-2) and Interleukin-6 (IL-6) (Figure 4C-1 and 2) increased in the lung of LPS-stimulated mice in

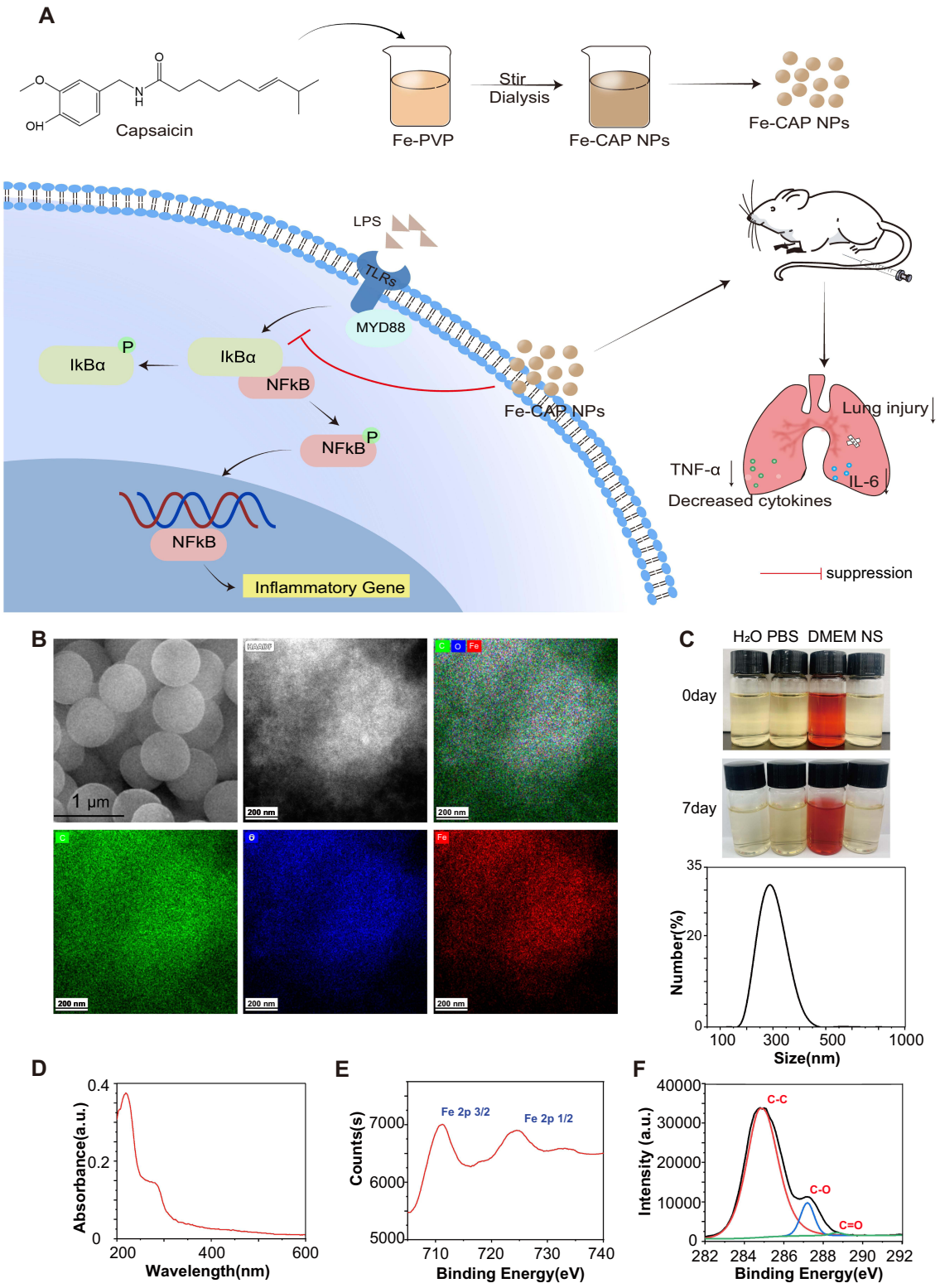

Figure 1 Synthesis and characterization of Fe-CAP NPs. Synthesis of Fe-CAP NPs and Fe-CAP NPs based treatment for ALI in mice (**A**). SEM of Fe-CAP NPs and TEM mapping of Fe-CAP NPs, showing the major elements in the nanoparticles (**B**). Hydrodynamic diameter distribution of Fe-CAP NPs in DLS measurements. Photos of Fe-CAP NPs dispersed in different media including H_2O, phosphate buffered saline (PBS), Dulbecco's Modified Eagle Medium (DMEM) and normal saline (NS) and for 7 days (**C**). UV spectra of Fe-CAP NPs (**D**). XPS spectra of Fe and C in Fe-CAP NPs, respectively (**E** and **F**).

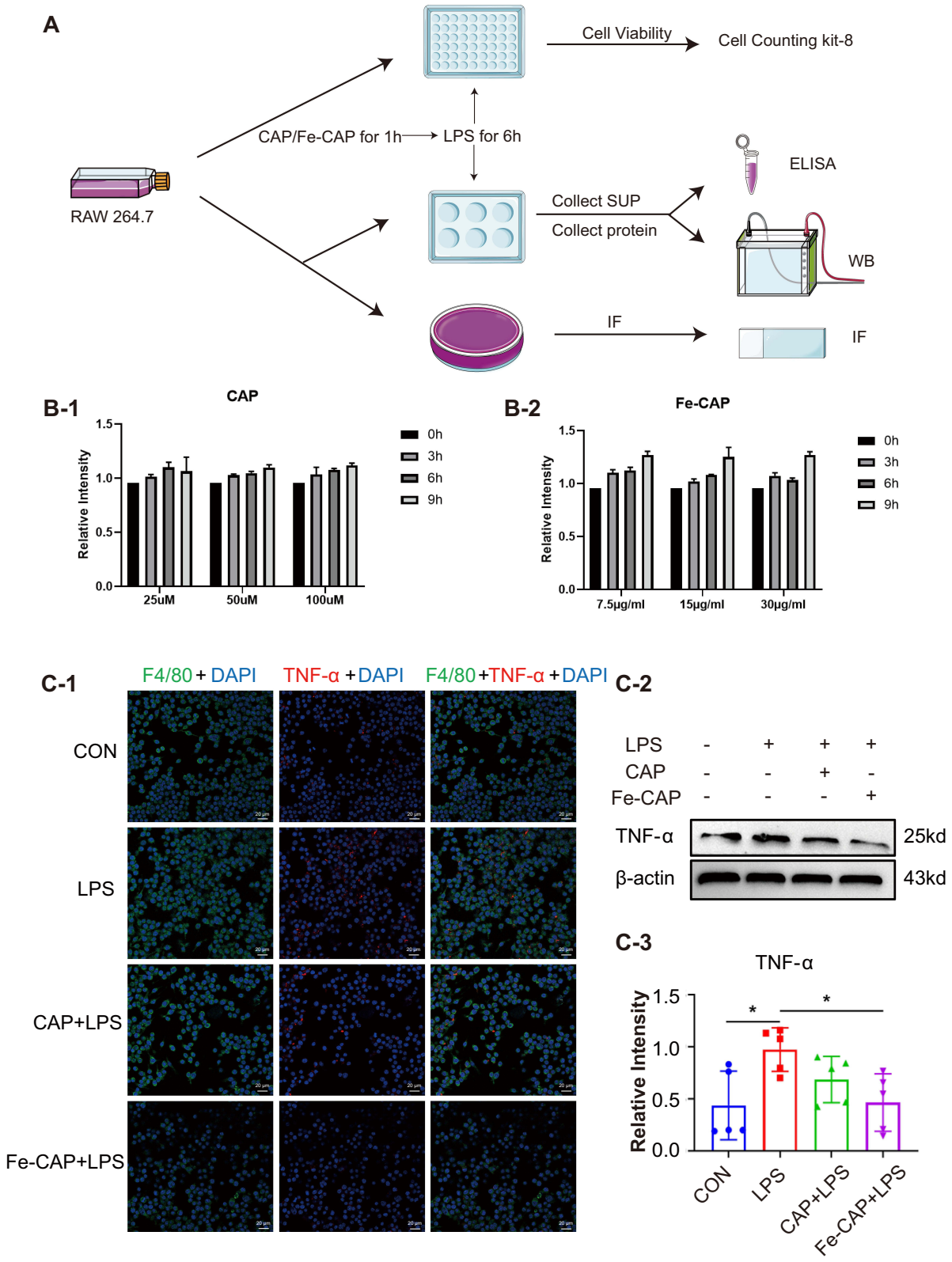

Figure 2 Anti-inflammatory effect of Fe-CAP NPs on LPS-induced RAW 264.7 cells. Schematic illustration of the experiment conducted here (**A**). Effect of CAP (**B-1**) and Fe-CAP NPs (**B-2**) on viability of RAW 264.7. TNF-α level was detected by immunofluorescence (**C-1**) and Western Blot (**C-2** and **C-3**). *Represents p<0.05.

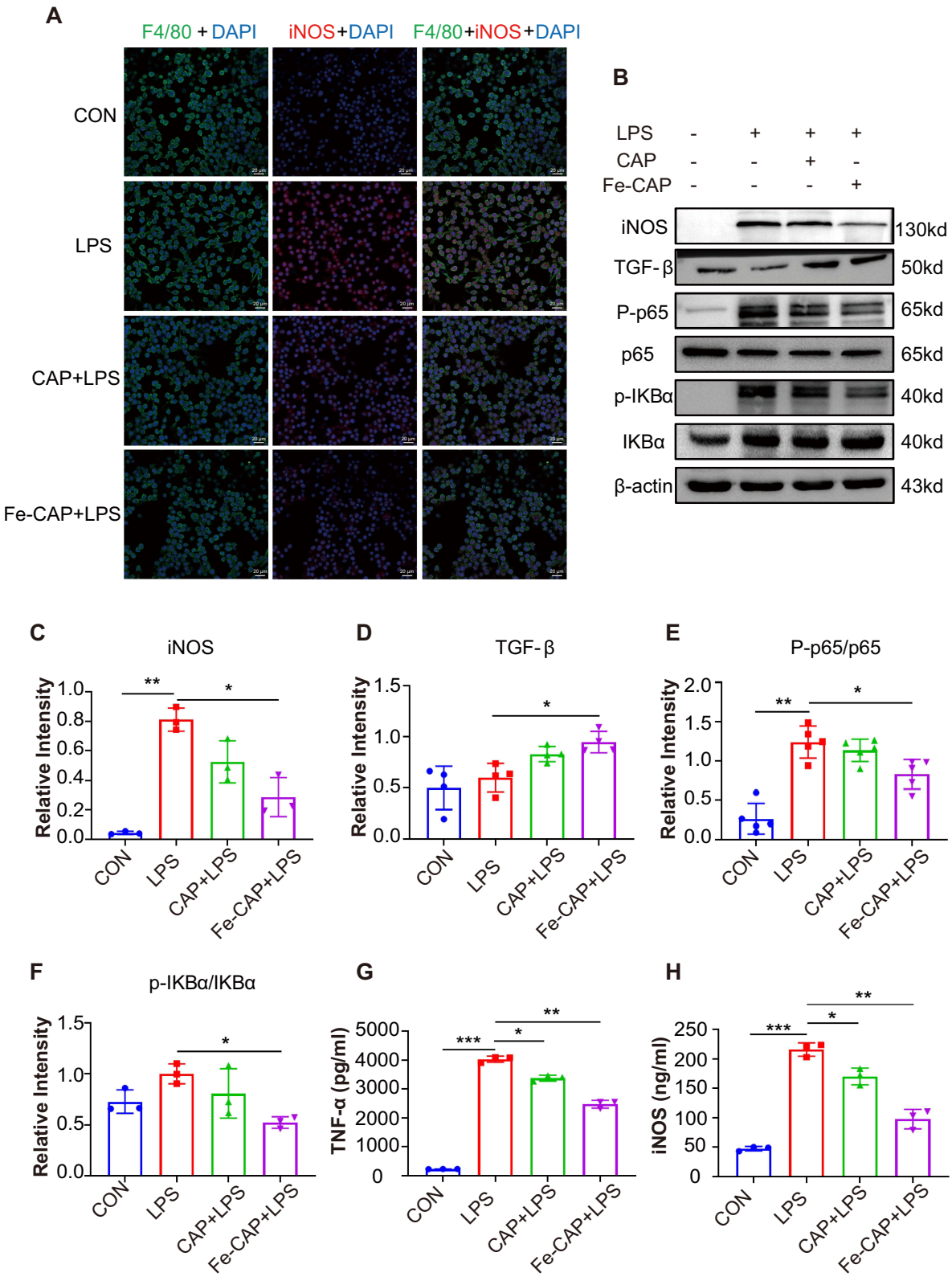

Figure 3 Anti-inflammatory effect of Fe-CAP NPs on LPS-induced RAW 264.7 cells. INOS levels were detected by immunofluorescence (**A**). INOS, TGF-β, p-NF-κB and p-IKBα levels were detected by Western Blot (**B**–**F**). TNF-α and iNOS levels were detected by ELISA (**G** and **H**). *Represents p<0.05, **Represents p<0.01, ***Represents p<0.001.

https://doi.org/10.2147/IJN.S436271 DovePress

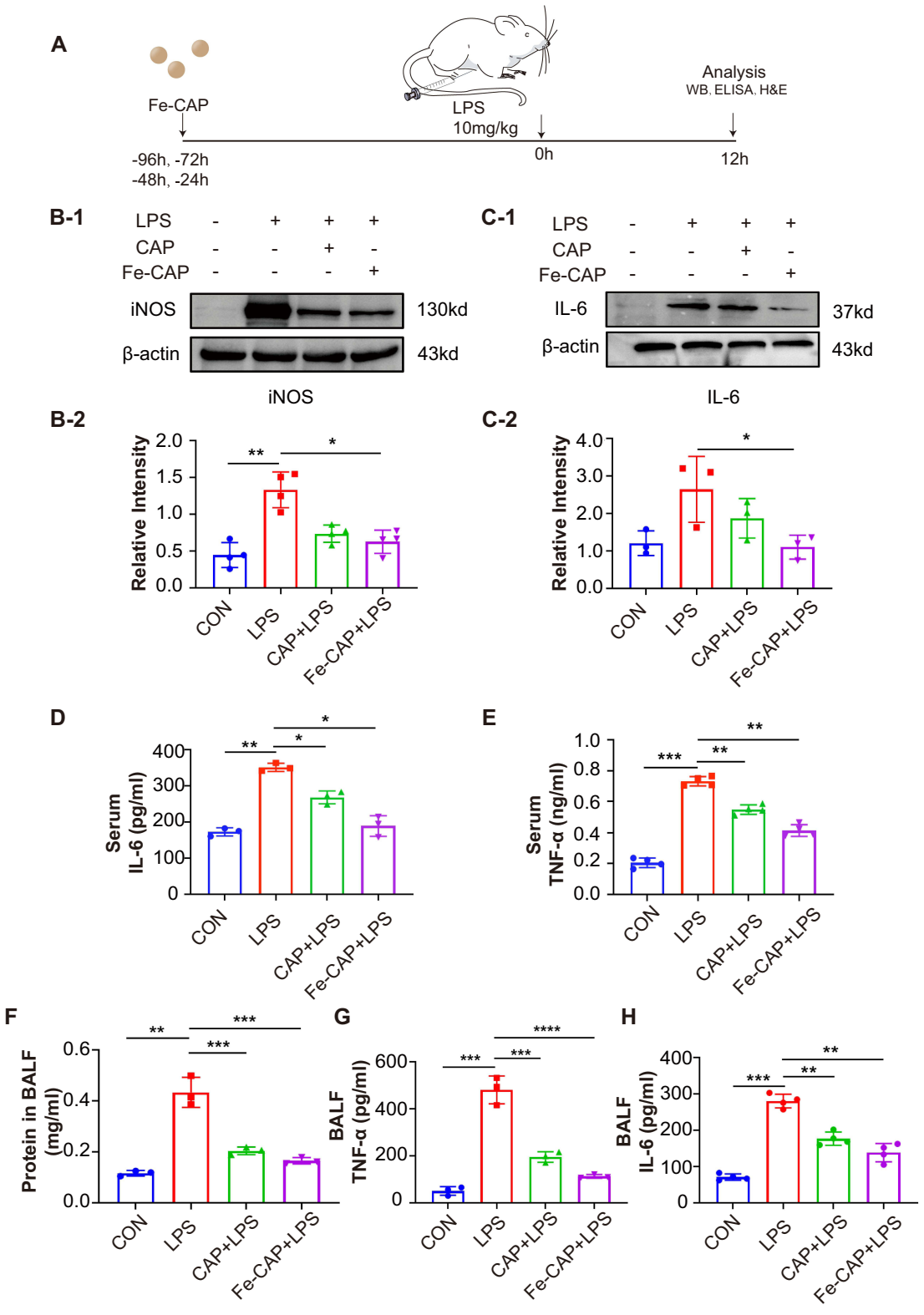

Figure 4 Anti-inflammatory effect of Fe-CAP NPs on mice. Schematic illustration of the establishment of the sepsis-related acute lung injury mouse model (**A**). The iNOS (**B-1** and **B-2**) and IL-6 (**C-1** and **C-2**) levels in the lung tissue of mice were detected by Western Blot. IL-6 and TNF-α level in serum of mice were detected by ELISA (**D** and **E**). The total protein concentrations in BALF of mice were measured using BCA assay kit (**F**). TNF-α and IL-6 level in BALF of mice were detected by ELISA (**G** and **H**). *represents p<0.05, **Represents p<0.01, ***Represents p<0.001, ****Represents p<0.0001.

comparison with sham, while Fe-CAP NPs pretreatment effectively decreased their expression. ELISA detection of the serum of mice and BALF of mice showed that the expression of inflammatory factors TNF-α (Figure 4E and G) and IL-6 (Figure 4D and H) in the LPS group increased, while the serum of mice and BALF of mice pretreated with Fe-CAP significantly decreased, and the effect was better than that of CAP group alone. Immunohistochemistry showed similar trend in the expression of TNF-α and IL-6 (Figure 5C). Total BALF protein levels (Figure 4F) increased in LPS group, while Fe-CAP NPs pretreatment decreased.

Fe-CAP NPs Alleviated Histopathological Alterations and Lung Injury Score

The lung tissues of different groups of mice were stained with hematoxylin and eosin (H&E). Lung sections showed obvious pathological changes in LPS group tissues, mainly manifested as thickened alveolar septum, obvious alveolar collapse, interstitial hemorrhage, large infiltration of lymphocytes and neutrophils in the interstitium, and high LIS (Figure 5A and B). However, after Fe-CAP treatment, lung tissue inflammation and destruction were reduced, and the effect of that treatments was better than that of CAP treatment alone.

Fe-CAP NPs Relieved Pulmonary Capillary Endothelial Leakage and Reduced the W/D Weight Ratio

The Evans blue extravasation of the LPS group was notably higher than that of the other groups. Extravasation decreased after CAP treatment, but the effect was better in Fe-CAP treatment group (Figure 5D-1 and D-2). Similarly, the W/D ratio of the lungs in the LPS group was obviously higher than that of the control group. After Fe-CAP pretreatment, the W/D ratio was lower than that of the CAP treatment group (Figure 5E).

Biosafety Evaluation of Fe-CAP NPs

Schematic illustration of toxicity in vivo is in Figure 6A. The results showed that the routine blood, liver function and renal function data were normal in mice treated with Fe-CAP NPs (Figures 6B and 7A). There were no significant differences between the groups. Through the utilisation of H&E staining imaging, it was observed that Fe-CAP NPs exhibited minimal toxicity to vital organs such as the heart, liver, spleen, lungs, and kidneys (Figure 7B). These results together demonstrated the efficacy and safety of Fe-CAP NPs in the treatment of ALI.

Discussion

Sepsis is a life-threatening organ dysfunction that results from a dysfunctional host response to infection, with an extremely high mortality rate.[28,29] In recent years, many drugs have been proved to be able to treat sepsis and relieve inflammation, but the treatment effect is not satisfactory. Capsaicin, a naturally active compound found in capsicum, has been shown to possess analgesic, antioxidant, and anti-tumor effects.[30,31] However, capsaicin also has certain deficiencies, such as poor water solubility, potential respiratory inhibition and induction of splenic and gastric damage with excessive use.[32] Currently, the precise mechanisms by which capsaicin exerts its therapeutic effects in sepsis remain unclear.

In recent years, nanozymes have gained significant attention due to their stability, validity and high enzyme activity.[33,34] Additionally, single-atom nanozymes have emerged as important tools in the field of biomedicine.[35–38] Metal-based nanozymes with Cu, Fe, Co, Mn and other materials have come into the human field of vision.[39] Xu et al synthesized carbon nanoparticles with zinc as the centre, which can catalyse the decomposition of hydrogen peroxide to produce hydroxyl free radicals, inhibit the growth of Pseudomonas aeruginosa, and promote wound healing.[37] Wang et al constructed a nanozyme with Cu atoms as the active centre for photothermal antimicrobial research.[40] Zhang et al synthesized novel manganese-iron dual single-atom catalysts (Mn/Fe SACs) to promote wound healing by modulating macrophage polarization into the anti-inflammatory M2 type.[41] Among the diverse nanocatalysts, iron-based biocatalysts have received special attention in diagnosis and disease treatment.[42] Studies have shown that iron-based nanozymes can be used to treat Alzheimer's disease and cardiovascular diseases, and can also act as anti-inflammatory agents to protect cells from ROS damage.[43] Given these considerations, we synthesized Fe-CAP NPs and conducted further research.

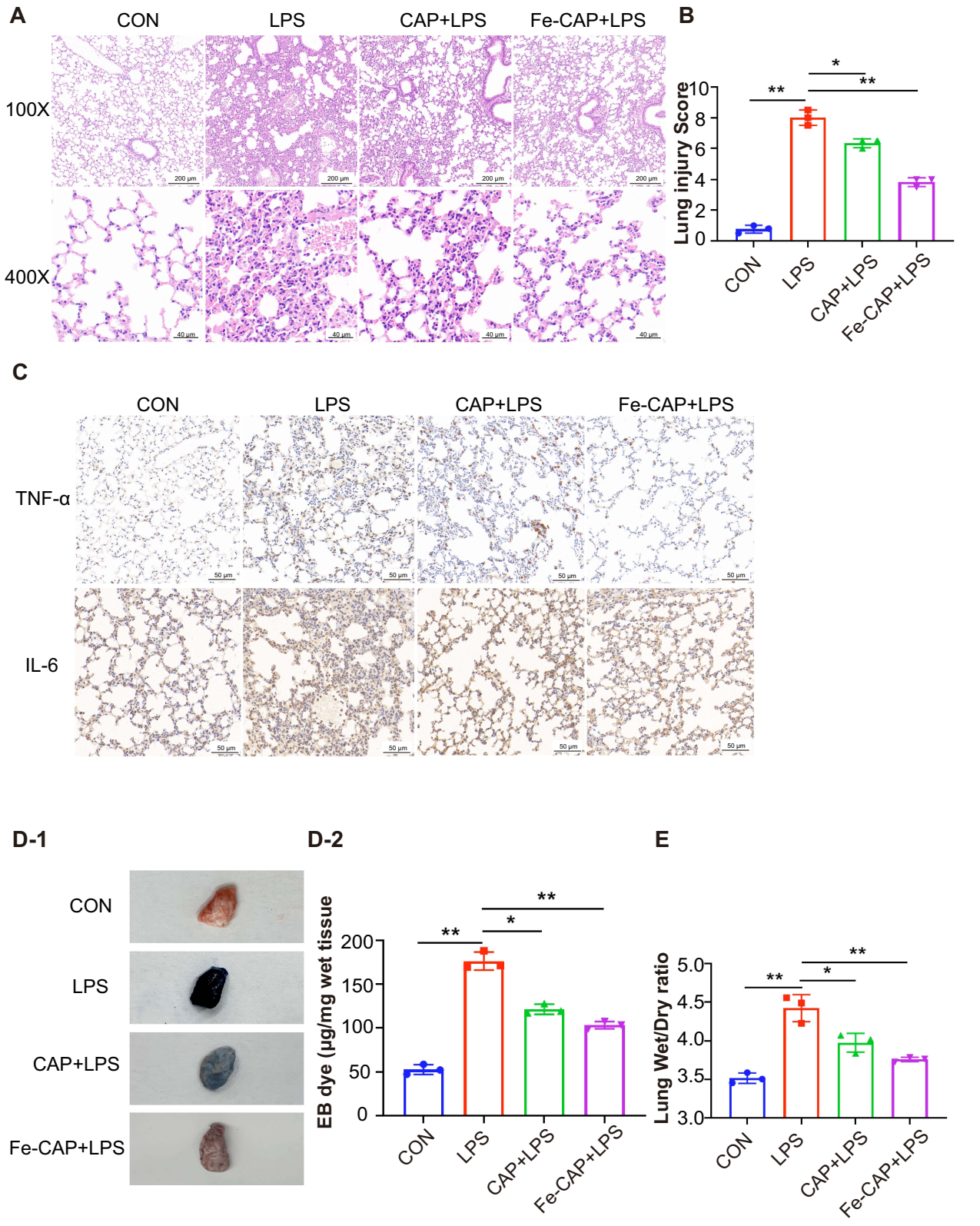

Figure 5 Fe-CAP NPs repaired the barrier structure and relieved pulmonary capillary endothelial leakage in LPS-Induced mouse lungs. Histopathological morphology was assessed by hematoxylin and eosin staining (**A**). After H&E staining, the lung injury score was performed blind by three pathologists (**B**). TNF-α and IL-6 level in lung tissue of mice were detected by immunohistochemistry (**C**). Pulmonary capillary endothelial leakage in lung tissue was detected by Evans Blue (**D-1** and **D-2**). Mouse lungs were weighed to calculated Lung Wet/Dry ratio (**E**). *Represents $p<0.05$, **Represents $p<0.01$.

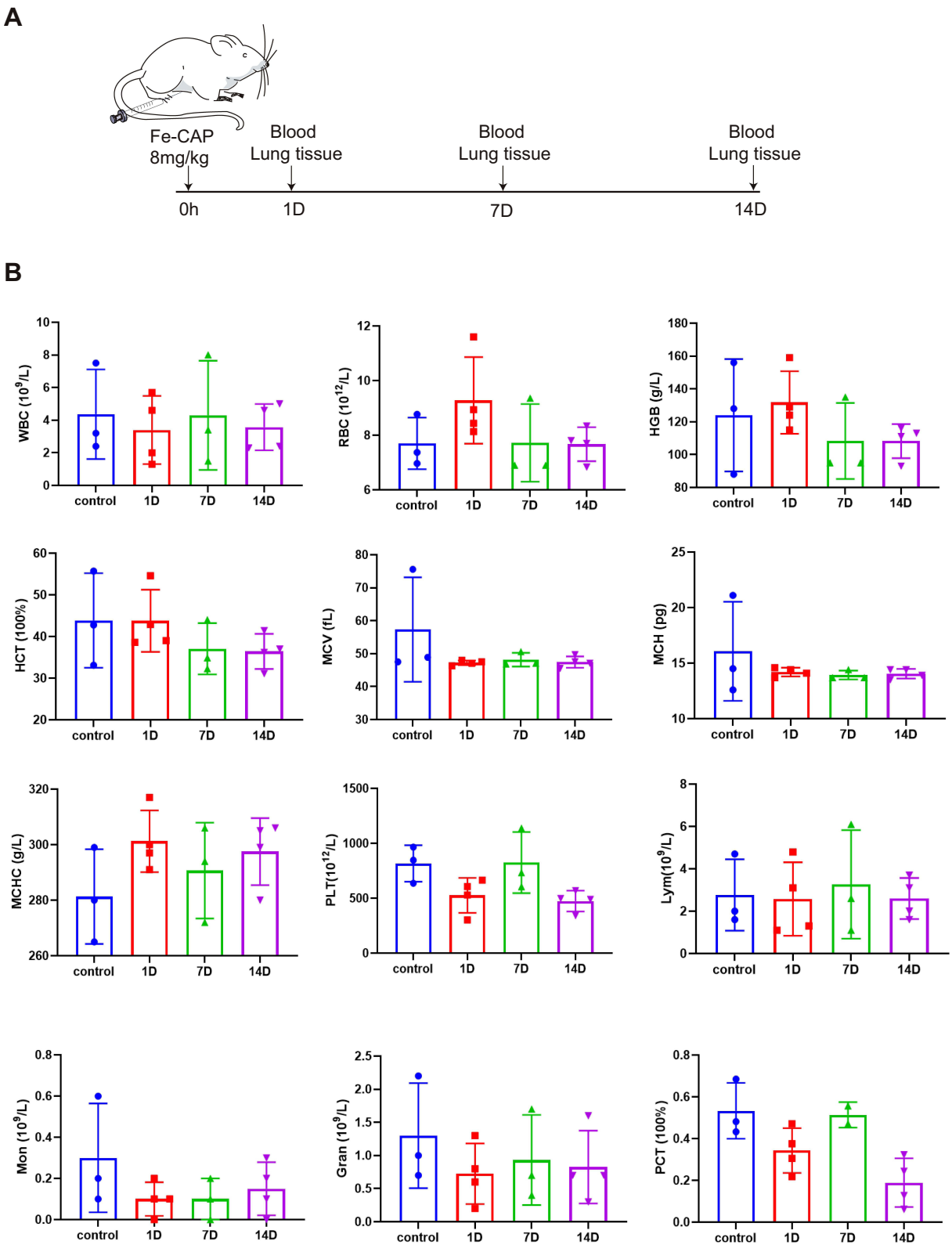

Figure 6 Toxicity of Fe-CAP NPs in vivo. Schematic illustration of toxicity in vivo (**A**). Blood panel data of normal mice (blank) and mice post Fe-CAP NPs injection at different time points (1, 7 and 14 days) (**B**).

https://doi.org/10.2147/IJN.S436271 DovePress

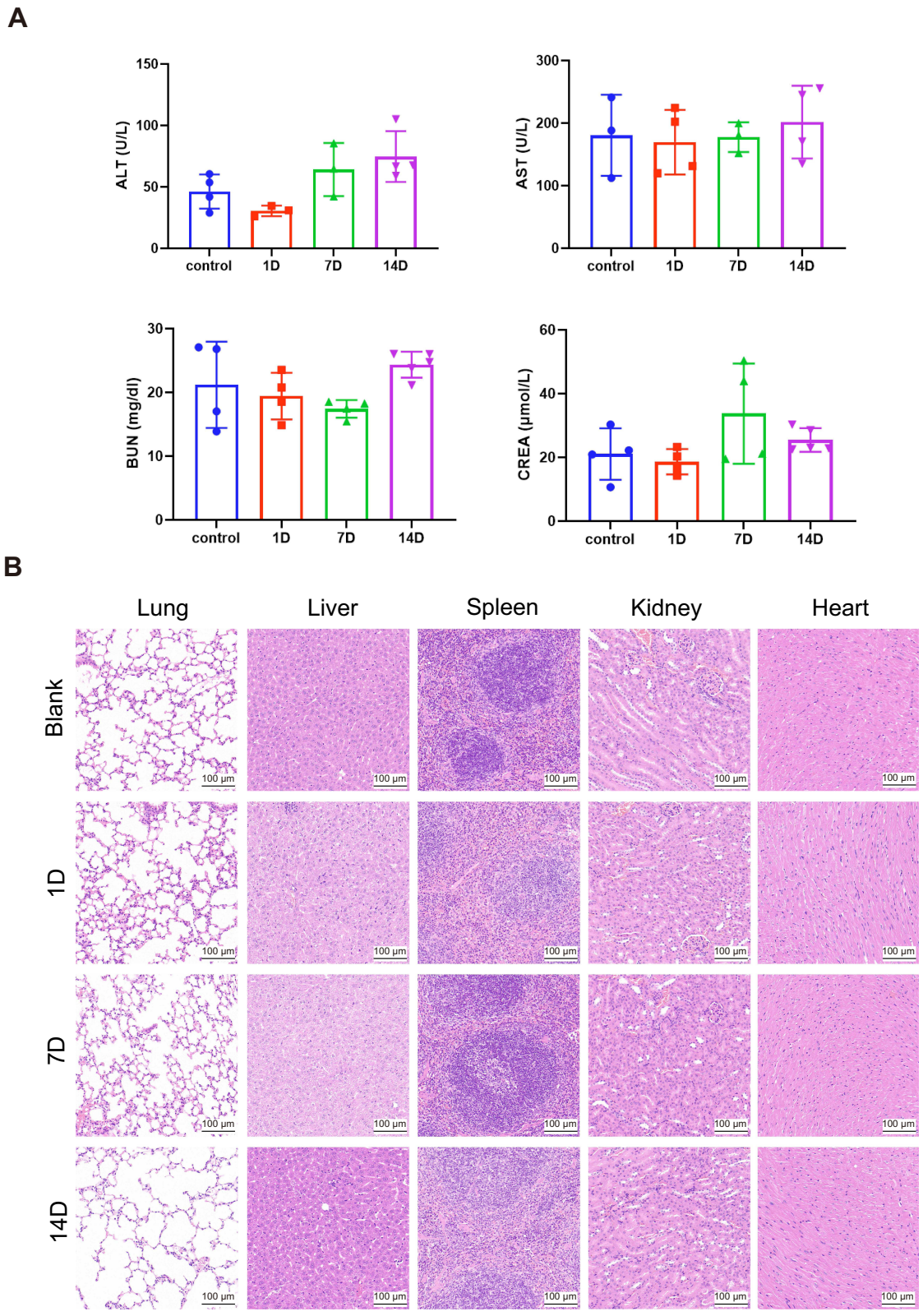

Figure 7 In vivo biosafety validation of Fe-CAP NPs. Liver and renal function analysis of blood in mice at 1, 7 and 14 days after administration of Fe-CAP NPs (**A**). H&E staining images of the major organs (lung, liver, spleen, kidney and heart) collected from the mice after injection of Fe-CAP NPs for 1, 7 and 14 days (**B**).

Characterization of Fe-CAP NPs showed that the synthesized nanozyme contains iron and capsaicin, and the three elements were evenly distributed. There were no aggregates in different media, which indicated that the Fe-CAP NPs had good colloidal stability. The above results demonstrated that we have successfully synthesized the Fe-CAP NPs. Next, we further explored the relevant mechanisms of nanozyme treatment of ALI.

The secretion of TNF-α is markedly increased in ALI. Studies have shown that blocking TNF-α receptors may protect endothelial cells and reduce the damage of tight junction proteins, thus alleviating ALI.[44] Macrophages are the main source of TNF-α in the lung.[45] Our experimental results showed that the expression of the inflammatory factors TNF-α and iNOS were decreased significantly after Fe-CAP NPs treatment, which was better than the effect of CAP treatment alone. Accordingly, the secretion of anti-inflammatory factor TGF-β was decreased in the LPS group but significantly increased after Fe-CAP pretreatment. Chen et al confirmed that capsaicin conferred protection against LPS-induced inflammation in RAW 264.7 cells. After LPS stimulation, the RAW 264.7 cells iNOS expression level increased significantly. Conversely, the expression of iNOS was markedly inhibited after capsaicin pretreatment.[24] Zhang et al found that capsaicin pretreatment can significantly inhibit LPS-induced inflammation in RAW 264.7 cells.[46] This is consistent with our findings. These results indicate that Fe-CAP NPs have a better anti-inflammatory effect and are more efficacious than capsaicin alone.

NF-κB is considered pivotal regulator of inflammation and plays a crucial role in controlling various aspects of the inflammatory response.[47–49] Chen et al demonstrated that Losartan modulated macrophage polarization through TLR4-mediated NF-κB signaling, thereby alleviating sepsis-induced cardiomyopathy.[50] Notably, the severity and mortality of ALI/ARDS caused by pneumonia or sepsis are primarily associated with NF-κB-mediated "cytokine storms".[51,52] To investigate the mechanism by which Fe-CAP NPs reduce LPS-induced inflammation in sepsis, we examined the effect of Fe-CAP NPs on the NF-κB signaling pathway. Western blot showed that NF-κB expression increased significantly after LPS stimulation and gradually returned to normal after Fe-CAP or CAP administration, which also verified the anti-inflammatory effect of this nanozyme.

Furthermore, we performed further verification in mice. The results demonstrated that Fe-CAP NPs intervention could effectively reduce the secretion of inflammatory factors, ameliorate the destruction of pulmonary endothelial cells, and alleviate pulmonary capillary leakage after LPS injection in mice. Specifically, Fe-CAP treatment in LPS-induced mice resulted in a decrease in the wet-to-dry (W/D) weight ratio and lung Evans blue secretion, as well as an amelioration of histopathological changes and lung injury scores, with a superior therapeutic effect compared to capsaicin alone. Yuan et al found that curcumin treatment had a certain alleviating effect on lung tissue lesions in mice with sepsis, and the alveolar structure was restored to a large extent.[42] The experiments in vivo further confirmed the anti-inflammatory effect of Fe-CAP, accompanied by structural changes in endothelial cells, which also confirmed the results of our cell experiments. The toxicity test in mice showed that Fe-CAP was safe and effective.

In conclusion, our findings provide evidence of the anti-inflammatory effect of Fe-CAP NPs on RAW 264.7 cells mediated through NF-κB signaling pathway. However, there are still some limitations to this study. The research on the anti-inflammatory mechanism of Fe-CAP NPs is not thorough enough, such as whether Fe-CAP NPs can play an anti-inflammatory role by regulating the phenotypic transformation of macrophages and whether Fe-CAP NPs can remove oxygen free radicals. This also needs to be further verified.

Conclusion

In summary, this study provides strong biochemical, morphological and experimental evidence that Fe-CAP NPs alleviate inflammation by inhibiting the expression of pro-inflammatory cytokines in macrophages, increasing the expression of anti-inflammatory cytokines, and alleviating the destruction of lung tissue structure.

Abbreviations

LPS, Lipopolysaccharide; Elisa, Enzyme-linked immunosorbent assay; NF-κB, Nuclear factor kappa-B; W/D, Wet-to-dry; ICU, Intensive care units; ARDS, Acute respiratory distress syndrome; Fe-CAP NPs, Iron-capsaicin-based nanoparticles; iNOS, Inducible nitric oxide synthase; IL-6, Interleukin-6; PVP, Polyvinylpyrrolidone; TNF-α, Tumor Necrosis Factor-α; TGF-β, Transforming Growth Factor-β; PBS, Phosphate-Buffered Saline; DMEM, Dulbecco's Modified Eagle Medium;

FBS, Fetal Bovine Serum; CCK-8, Cell Counting Kit 8; BCA, Bicinchoninic acid; EB, Exosmotic Evans Blue; LIS, The Lung Injury Score; i.p., Intraperitoneal; TEM, Transmission electron microscopy; SEM, Scanning electron microscope; XPS, X-ray photoelectron spectroscopy; MODS, Multiple organ dysfunction syndrome.

Acknowledgments

The authors thank the Chinese Academy of Medical Sciences for the support.

Author Contributions

All authors made a significant contribution to the work reported, whether that is in the conception, study design, execution, acquisition of data, analysis and interpretation, or in all these areas; took part in drafting, revising or critically reviewing the article; gave final approval of the version to be published; have agreed on the journal to which the article has been submitted; and agree to be accountable for all aspects of the work.

Funding

This study was funded by CAMS Innovation Fund for Medical Sciences (2019-I2M-5-023), National Natural Science Foundation of China (82303712), China Postdoctoral Science Foundation (2023M740520),Hainan Provincial Key Research and Development Project (ZDYF2020112) and Finance Science and Technology Program of Sichuan Province (2022YFS0602).

Disclosure

The authors declare that they have no competing financial interest conflicts or personal relationships in this work.

References

1. Hudson L, Steinberg K. Epidemiology of acute lung injury and ARDS. *Chest*. 1999;116:74S–82S. doi:10.1378/chest.116.suppl_1.74S-a
2. Navegantes-Lima K, Monteiro V, de França Gaspar S, et al. Agaricus brasiliensis mushroom protects against sepsis by alleviating oxidative and inflammatory response. *Front Immunol*. 2020;11:1238. doi:10.3389/fimmu.2020.01238
3. Rudd K, Johnson S, Agesa K, et al. Global, regional, and national sepsis incidence and mortality, 1990–2017: analysis for the global burden of disease study. *Lancet*. 2020;395(10219):200–211. doi:10.1016/S0140-6736(19)32989-7
4. Esposito S, De Simone G, Boccia G, De Caro F, Pagliano P. Sepsis and septic shock: new definitions, new diagnostic and therapeutic approaches. *J Global Antimicrob Resist*. 2017;10:204–212. doi:10.1016/j.jgar.2017.06.013
5. Singer M, Deutschman C, Seymour C, et al. The third international consensus definitions for sepsis and septic shock (Sepsis-3). *JAMA*. 2016;315(8):801–810. doi:10.1001/jama.2016.0287
6. Mayr F, Yende S, Angus D. Epidemiology of severe sepsis. *Virulence*. 2014;5(1):4–11. doi:10.4161/viru.27372
7. He Y, Zhou C, Yu L, et al. Natural product derived phytochemicals in managing acute lung injury by multiple mechanisms. *Pharmacol Res*. 2021;163:105224. doi:10.1016/j.phrs.2020.105224
8. Thompson BT, Chambers RC, Liu KD. Acute respiratory distress syndrome. *N Engl J Med*. 2017;377(6):562–572. doi:10.1056/NEJMra1608077
9. Qiao Q, Liu X, Yang T, et al. Nanomedicine for acute respiratory distress syndrome: the latest application, targeting strategy, and rational design. *Acta pharmaceutica Sinica B*. 2021;11(10):3060–3091.
10. Hsieh Y, Deng J, Pan H, Liao J, Huang S, Huang G. Sclareol ameliorate lipopolysaccharide-induced acute lung injury through inhibition of MAPK and induction of HO-1 signaling. *Int Immunopharmacol*. 2017;44:16–25. doi:10.1016/j.intimp.2016.12.026
11. Kolomaznik M, Nova Z, Calkovska A. Pulmonary surfactant and bacterial lipopolysaccharide: the interaction and its functional consequences. *Physiol Res*. 2017;66:S147–S157.
12. Bae H, Li M, Kim J, et al. The effect of epigallocatechin gallate on lipopolysaccharide-induced acute lung injury in a murine model. *Inflammation*. 2010;33(2):82–91. doi:10.1007/s10753-009-9161-z
13. Kim C, Kawada T, Kim B, et al. Capsaicin exhibits anti-inflammatory property by inhibiting IkB-a degradation in LPS-stimulated peritoneal macrophages. *Cell. Signalling*. 2003;15(3):299–306. doi:10.1016/S0898-6568(02)00086-4
14. Borghi S, Carvalho T, Staurengo-Ferrari L, et al. Vitexin inhibits inflammatory pain in mice by targeting TRPV1, oxidative stress, and cytokines. *J Natural Prod*. 2013;76(6):1141–1149. doi:10.1021/np400222v
15. Uhelski M, McAdams B, Johns M, Kabadi R, Simone D, Banik R. Lack of relationship between epidermal denervation by capsaicin and incisional pain behaviours: a laser scanning confocal microscopy study in rats. *Europ J Pain*. 2020;24(6):1197–1208. doi:10.1002/ejp.1564
16. Hughes S, Ward G, Strutton P. Anodal transcranial direct current stimulation over the primary motor cortex attenuates capsaicin-induced dynamic mechanical allodynia and mechanical pain sensitivity in humans. *Europ J Pain*. 2020;24(6):1130–1137. doi:10.1002/ejp.1557
17. Lu H, Chen Y, Yang J, et al. Antitumor activity of capsaicin on human colon cancer cells in vitro and colo 205 tumor xenografts in vivo. *J Agricul Food Chem*. 2010;58(24):12999–13005. doi:10.1021/jf103335w
18. Shen S, Li H, Chen K, et al. Spatial targeting of tumor-associated macrophages and tumor cells with a pH-Sensitive cluster nanocarrier for cancer chemoimmunotherapy. *Nano Lett*. 2017;17(6):3822–3829. doi:10.1021/acs.nanolett.7b01193

19. Wang D, Wu H, Yang G, et al. Metal-organic framework derived multicomponent nanoagent as a reactive oxygen species amplifier for enhanced photodynamic therapy. *ACS nano*. 2020;14(10):13500–13511. doi:10.1021/acsnano.0c05499
20. Li C, Hang T, Jin Y. Atomically Fe-anchored MOF-on-MOF nanozyme with differential signal amplification for ultrasensitive cathodic electrochemiluminescence immunoassay. *Exploration*. 2023;3(4):20220151. doi:10.1002/EXP.20220151
21. Ren X, Chen D, Wang Y, et al. Nanozymes-recent development and biomedical applications. *J Nanobiotechnol*. 2022;20(1):92. doi:10.1186/s12951-022-01295-y
22. Zhu Z, Lu H, Jin L, et al. C-176 loaded Ce DNase nanoparticles synergistically inhibit the cGAS-STING pathway for ischemic stroke treatment. *Bioact Mater*. 2023;29:230–240. doi:10.1016/j.bioactmat.2023.07.002
23. Liang M, Yan X. Nanozymes: from new concepts, mechanisms, and standards to applications. *Acc Chem Res*. 2019;52(8):2190–2200. doi:10.1021/acs.accounts.9b00140
24. Chen K, Chen P, Hsieh Y, Lin C, Lee Y, Chu S. Capsaicin protects endothelial cells and macrophage against oxidized low-density lipoprotein-induced injury by direct antioxidant action. *Chem Biol Interact*. 2015;228:35–45. doi:10.1016/j.cbi.2015.01.007
25. Lai K, Song C, Gao M, et al. Uridine alleviates sepsis-induced acute lung injury by inhibiting ferroptosis of macrophage. *Int J Mol Sci*. 2023;24(6):5093. doi:10.3390/ijms24065093
26. Carrascal M, Areny-Balaguero A, de-Madaria E, et al. Inflammatory capacity of exosomes released in the early stages of acute pancreatitis predicts the severity of the disease. *J Pathol*. 2022;256(1):83–92. doi:10.1002/path.5811
27. Matute-Bello G, Downey G, Moore B, et al. An official American thoracic society workshop report: features and measurements of experimental acute lung injury in animals. *Am J Respir Cell Mol Biol*. 2011;44(5):725–738. doi:10.1165/rcmb.2009-0210ST
28. Druzak S, Iffrig E, Roberts B, et al. Multiplatform analyses reveal distinct drivers of systemic pathogenesis in adult versus pediatric severe acute COVID-19. *Nat Commun*. 2023;14(1):1638. doi:10.1038/s41467-023-37269-3
29. Wang W, Liu C. Sepsis heterogeneity. *World J Pediat*. 2023;19(10):919–927. doi:10.1007/s12519-023-00689-8
30. Huang K, Chiang Y, Huang T, et al. Capsaicin alleviates cisplatin-induced muscle loss and atrophy in vitro and in vivo. *J Cachex Sarcop Musc*. 2023;14(1):182–197. doi:10.1002/jcsm.13120
31. Rollyson W, Stover C, Brown K, et al. Bioavailability of capsaicin and its implications for drug delivery. *J Controll Rele*. 2014;196:96–105. doi:10.1016/j.jconrel.2014.09.027
32. Merritt J, Richbart S, Moles E, et al. Anti-cancer activity of sustained release capsaicin formulations. *Pharmacol Ther*. 2022;238:108177. doi:10.1016/j.pharmthera.2022.108177
33. Mohammadi Z, Zhang F, Kharazmi M, Jafari S. Nano-biocatalysts for food applications; immobilized enzymes within different nanostructures. *Crit Rev Food Sci Nutr*. 2022;2022:1–19.
34. Jin L, Cao F, Gao Y, et al. Microenvironment-activated nanozyme-armed bacteriophages efficiently combat bacterial infection. *Advan Mater*. 2023;35:30.
35. Li Y, Wang Y, Dong C, et al. Single-atom nickel terminating sp and sp nitride in polymeric carbon nitride for visible-light photocatalytic overall water splitting. *Chem Sci*. 2021;12(10):3633–3643. doi:10.1039/D0SC07093A
36. Sun T, Mitchell S, Li J, et al. Design of local atomic environments in single-atom electrocatalysts for renewable energy conversions. *Advan Mater*. 2021;33(5):e2003075. doi:10.1002/adma.202003075
37. Xu B, Wang H, Wang W, et al. A single-atom nanozyme for wound disinfection applications. *Angew Chem*. 2019;58(15):4911–4916. doi:10.1002/anie.201813994
38. Cao F, Jin L, Gao Y, et al. Artificial-enzymes-armed Bifidobacterium longum probiotics for alleviating intestinal inflammation and microbiota dysbiosis. *Nature Nanotechnol*. 2023;18(6):617–627. doi:10.1038/s41565-023-01346-x
39. Yang Z, Guo J, Wang L, et al. Nanozyme-enhanced electrochemical biosensors: mechanisms and applications. *Small*;2023. e2307815. doi:10.1002/smll.202307815
40. Wang X, Shi Q, Zha Z, et al. Copper single-atom catalysts with photothermal performance and enhanced nanozyme activity for bacteria-infected wound therapy. *Bioact Mater*. 2021;6(12):4389–4401. doi:10.1016/j.bioactmat.2021.04.024
41. Zhang M, Xu W, Gao Y, Zhou N, Wang W. Manganese-iron dual single-atom catalyst with enhanced nanozyme activity for wound and pustule disinfection. *ACS Appl Mater Interfaces*. 2023;15(36):42227–42240. doi:10.1021/acsami.3c08018
42. Yuan R, Li Y, Han S, et al. Fe-curcumin nanozyme-mediated reactive oxygen species scavenging and anti-inflammation for acute lung injury. *ACS Cent. Sci.* 2022;8(1):10–21. doi:10.1021/acscentsci.1c00866
43. Shi C, Li Y, Gu N. Iron-based nanozymes in disease diagnosis and treatment. *Chembiochem*. 2020;21(19):2722–2732. doi:10.1002/cbic.202000094
44. Fang M, Zhong W, Song W, et al. Ulinastatin ameliorates pulmonary capillary endothelial permeability induced by sepsis through protection of tight junctions via inhibition of TNF-α and related pathways. *Front Pharmacol*. 2018;9:823. doi:10.3389/fphar.2018.00823
45. Wang R, Song W, Xie C, et al. Urinary trypsin inhibitor protects tight junctions of septic pulmonary capillary endothelial cells by regulating the functions of macrophages. *J Inflamm Res*. 2021;14:1973–1989. doi:10.2147/JIR.S303577
46. Zhang Q, Luo P, Xia F, et al. Capsaicin ameliorates inflammation in a TRPV1-independent mechanism by inhibiting PKM2-LDHA-mediated Warburg effect in sepsis. *Cell Chem Biol*. 2022;29(8):1248–1259.e1246. doi:10.1016/j.chembiol.2022.06.011
47. Zhang Q, Lenardo M, Baltimore D. 30 Years of NF-κB: a blossoming of relevance to human pathobiology. *Cell*. 2017;168:37–57. doi:10.1016/j.cell.2016.12.012
48. Tiruppathi C, Soni D, Wang D, et al. The transcription factor DREAM represses the deubiquitinase A20 and mediates inflammation. *Nat Immunol*. 2014;15(3):239–247. doi:10.1038/ni.2823
49. Wertz I, O'Rourke K, Zhou H, et al. De-ubiquitination and ubiquitin ligase domains of A20 downregulate NF-kappaB signalling. *Nature*. 2004;430:7000):694–699. doi:10.1038/nature02794
50. Chen X, Wang S, Liu C, et al. Losartan attenuates sepsis-induced cardiomyopathy by regulating macrophage polarization via TLR4-mediated NF-κB and MAPK signaling. *Pharmacol Res*. 2022;185:106473. doi:10.1016/j.phrs.2022.106473
51. Chousterman B, Swirski F, Weber G. Cytokine storm and sepsis disease pathogenesis. *Semin Immunopathol*. 2017;39(5):517–528. doi:10.1007/s00281-017-0639-8
52. Fajgenbaum D, June C. Cytokine Storm. *N Engl J Med*. 2020;383(23):2255–2273. doi:10.1056/NEJMra2026131